

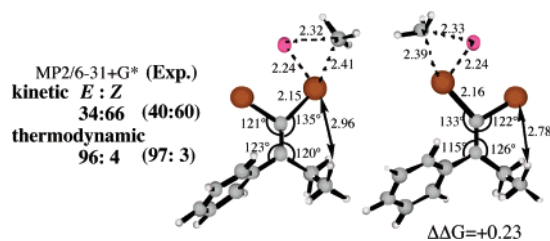
## Theoretical Study on the Lithium–Halogen Exchange Reaction of 1,1-Dihaloalkenes with Methyllithium and the Nucleophilic Substitution Reaction of the Resulting $\alpha$ -Halo Alkenyllithiums

Kaori Ando

College of Education, University of the Ryukyus, Nishihara-cho, Okinawa 903-0213, Japan

ando@edu.u-ryukyu.ac.jp

Received September 20, 2005



Transition structures for the lithium–bromine exchange reaction of 1,1-dibromoalkenes with methyllithium have been located by both the B3LYP and the MP2 levels of theory with the 6-31+G\* basis set. The reaction with methyllithium dimer gave similar results with lower activation energies. These calculations predict both the kinetic and the thermodynamic stereoselectivity correctly. That is, the sterically more constrained bromine atom of 1,1-dibromoalkenes was predominantly reacted with alkyllithium (dimer) in the kinetic condition. The intramolecular substitution reaction of 4,4-dibromo-3-methyl-3-pentenol in the presence of methyllithium has been investigated. After deprotonation of the alcohol and the lithium–bromine exchange reaction, the intramolecular substitution reaction occurs to give dihydrofuran in a concerted manner. The intermolecular substitution of  $\alpha$ -chloro alkenyllithium with methyllithium was also studied for comparison. The formation of the indene derivative from 3-(*o*-bromophenyl)-1,1-dibromo-1-propene in the presence of methyllithium occurs in a similar manner. The lithium–bromine exchange reaction of bromobenzene with methyllithium occurs in an  $S_N2$  mechanism and the solvent plays an important role.

### Introduction

The  $\alpha$ -halo alkenyllithium compounds function as latent carbenes and they are grouped under the nonspecific term carbenoids. However, some of their reactions do not involve free carbenes. Since they have the  $sp^2$  carbon containing both the positive metal (lithium) and the negative leaving group (halogen), they react not only as electrophiles, but also as nucleophiles. After the pioneering work of Köbrich,<sup>1</sup> the interest in carbenoids has not diminished.<sup>2–7</sup> Although the reaction of the  $\alpha$ -halo alkenyllithium compounds is diverse,<sup>8–13</sup> their preparative scope has not been fully appreciated. The substitu-

tion reactions of  $\alpha$ -halo alkenyllithium compounds at the  $sp^2$  carbon were also studied and the inversion of the configuration was observed to a certain extent (39% ee) in the nucleophilic substitution of an optically active  $\alpha$ -halo alkenyllithium compound (eq 1, Scheme 1).<sup>14</sup> In addition, it was reported that benzofurans were obtained from *o*-hydroxy- $\beta,\beta$ -dichlorostyrenes

(1) Köbrich, G. *Angew. Chem., Int. Ed. Engl.* **1972**, *11*, 473–485 and references therein.

(2) Seebach, D.; Siegel, H.; Müllen, K.; Hiltbrunner, K. *Angew. Chem., Int. Ed.* **1979**, *18*, 784–785.

(3) (a) Seebach, D.; Siegel, H.; Gabriel, J.; Hässig, R. *Helv. Chim. Acta* **1980**, *63*, 2046–2053. (b) Seebach, D.; Hässig, R.; Gabriel, J. *Helv. Chim. Acta* **1983**, *66*, 308–337.

(4) Schleyer, P. v. R.; Clark, T.; Kos, A. J.; Spitznagel, G. W.; Rohde, C.; Arad, D.; Houk, K. N.; Rondan, N. G. *J. Am. Chem. Soc.* **1984**, *106*, 6467–6475.

(5) (a) Pratt, L. M.; Ramachandran, B.; Xidos, J. D.; Cramer, C. J.; Truhlar D. G. *J. Org. Chem.* **2002**, *67*, 7607–7612. (b) Pratt, L. M.; Nguyen, N. V.; Le, L. T. *J. Org. Chem.* **2005**, *70*, 2294–2298.

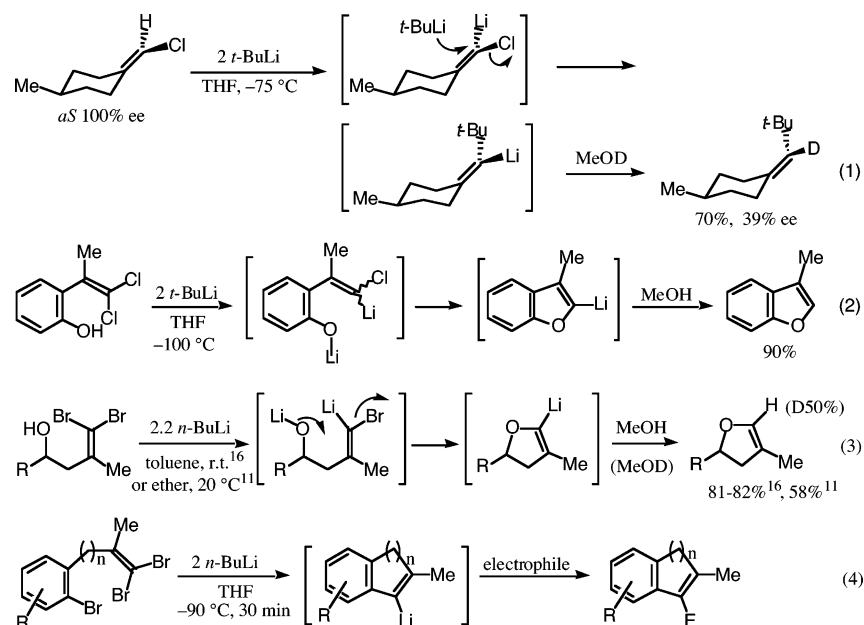
(6) Boche, G.; Marsch, M.; Müller, A.; Harms, K. *Angew. Chem., Int. Ed. Engl.* **1993**, *32*, 1032–1033.

(7) (a) Köbrich, G.; Ansari, F. *Chem. Ber.* **1967**, *100*, 2011–2020. (b) Boche, G.; Lohrenz, J. C. W. *Chem. Rev.* **2001**, *101*, 697–756.

(8) (a) Braun, M. *Angew. Chem., Int. Ed. Engl.* **37**, 430–451. (b) Kirmse, W. *Angew. Chem., Int. Ed. Engl.* **1997**, *36*, 1164–1170. (c) Oku, A. *J. Synth. Org. Chem., Jpn.* **1995**, *53*, 2–12.

(9) (a) Corey, E. J.; Fuchs, P. L. *Tetrahedron Lett.* **1972**, 3769–3772. (b) Eisler, S.; Tykwinski, R. R. *J. Am. Chem. Soc.* **2000**, *122*, 10736–10737.

## SCHEME 1



by the treatment with alkyllithium at  $-100\text{ }^{\circ}\text{C}$  (eq 2).<sup>15</sup> However, the inversion ratio is low and electron-transfer processes cannot be excluded. Narasaka and co-workers studied the intramolecular substitution reactions of  $\alpha$ -halo alkenyllithium compounds in detail (eq 3).<sup>11,16</sup> Their experiments excluded not only electron-transfer processes, but also the carbene insertion, addition–elimination, and allylic rearrangement for a major reaction pathway. On the basis of their results, the cyclization seems mostly to proceed by the in-plain  $\text{S}_{\text{N}}2$ -type mechanism.<sup>17</sup> They also applied this intramolecular substitution reaction to the regioselective preparation of indene derivatives (eq 4).<sup>16</sup> To better understand these intramolecular substitution reactions of  $\alpha$ -halo alkenyllithium compounds, we have studied the reaction mechanism computationally. A part of our theoretical study of this intramolecular substitution reaction has been published.<sup>16b</sup>

The most common method for generating  $\alpha$ -halo alkenyllithium compounds is the halogen–lithium exchange reaction of

1,1-dihaloalkenes with alkyllithiums. In general, the reaction rate decreases along the series  $\text{I} > \text{Br} > \text{Cl} \gg \text{F}$ . The halogen–metal exchange reaction has been the subject of numerous studies and mechanistic speculations. Four different mechanisms have been suggested for the halogen–metal exchange reaction:<sup>18</sup> (1) a stepwise process initiated by a single electron transfer, (2) a four-center reaction, (3) formation of an ate complex, and (4) an  $\text{S}_{\text{N}}2$  type mechanism (nucleophilic attack by  $\text{R}^-$  at halogen). Among them, the  $\text{S}_{\text{N}}2$  mechanism was suggested by kinetic studies of the aryl bromide–organolithium exchange reaction.<sup>19</sup> Furthermore, both experimental evaluation of transition structure geometry for an aryl bromide–alkyllithium exchange reaction by the *endo*-cyclic restriction test<sup>20</sup> and the stereospecific formation of  $\alpha$ -halo alkenyllithiums from *E*- and *Z*-bromochloroalkenes with retention of the configuration<sup>21a</sup> support either the intermediate ate complex or the  $\text{S}_{\text{N}}2$  mechanism.

Here, we would like to report full details of our theoretical study on the lithium–halogen exchange reaction of 1,1-dihaloalkenes with methylolithium and the nucleophilic substitution reaction of the resulting  $\alpha$ -halo alkenyllithium compounds.

### Method of Calculation

All calculations were performed with the Gaussian 98 program.<sup>22</sup> Gibbs free energies are the values at 1.00 atm obtained from the frequency calculations, which were done at several temperatures to obtain the thermal corrections to the activation free energies. Most of the calculations were performed by the B3LYP hybrid functional<sup>23</sup> together with the 6-31+G\* basis set. Since the scale factor for B3LYP/6-31+G\* is very close to 1.0,<sup>24</sup> the thermal energy corrections are not scaled. Vibrational frequency calculations gave only one imaginary

(10) (a) Harada, T.; Nozaki, Y.; Yamaura, Y.; Oku, A. *J. Am. Chem. Soc.* **1985**, *107*, 2189–2190. (b) Oku, A.; Harada, T.; Hattori, K.; Nozaki, Y.; Yamaura, Y. *J. Org. Chem.* **1988**, *53*, 3089–3098.

(11) Baird, M. S.; Baxter, A. G. W.; Hoorfar, A.; Jefferies, I. *J. Chem. Soc., Perkin Trans. 1* **1991**, 2575–2581.

(12) (a) Negishi, E.; Akiyoshi, K.; O'Connor, B.; Takagi, K.; Wu, G. *J. Am. Chem. Soc.* **1989**, *111*, 3089–3091. (b) Kasatkin, A.; Whitby, R. J. *J. Am. Chem. Soc.* **1999**, *121*, 7039–7049.

(13) (a) Pelter, A.; Kvicala, J.; Parry, D. E. *J. Chem. Soc., Perkin Trans. 1* **1995**, 2681–2682. (b) Wang, B.; Deng, C. *Chem. Phys. Lett.* **1988**, *147*, 99–104.

(14) (a) Duraisamy, M.; Walborsky, H. M. *J. Am. Chem. Soc.* **1984**, *106*, 5035–5037. (b) Topolski, M.; Duraisamy, M.; Rachon, J.; Gawronski, J.; Gawronska, K.; Goedken, V.; Walorsky, H. M. *J. Org. Chem.* **1993**, *58*, 546–555. (c) Rachon, J.; Goedken, V.; Walborsky, H. M. *J. Am. Chem. Soc.* **1986**, *108*, 7435–7436. (d) Topolski, M.; Walborsky, H. M. *J. Org. Chem.* **1994**, *59*, 5506–5510.

(15) (a) Topolski, M. *J. Org. Chem.* **1995**, *60*, 5588–5594. (b) A similar reaction of  $\alpha$ -lithiated cyclic enol ethers was reported: Nguyen, T.; Negishi, E. *Tetrahedron Lett.* **1991**, *32*, 5903–5906.

(16) (a) Yanagisawa, H.; Miura, K.; Kitamura, M.; Narasaka, K.; Ando, K. *Helv. Chim. Acta* **2002**, *85*, 3130–3135. (b) Yanagisawa, H.; Miura, K.; Kitamura, M.; Narasaka, K.; Ando, K. *Bull. Chem. Soc. Jpn.* **2003**, *76*, 2009–2026.

(17) For the in-plain  $\text{S}_{\text{N}}2$  reaction at the  $\text{sp}^2$  carbon, see: Ando, K.; Kitamura, M.; Miura, K.; Narasaka, K. *Org. Lett.* **2004**, *6*, 2461–2463 and references therein.

(18) Bailey, W. F.; Patricia, J. J. *J. Organomet. Chem.* **1988**, *352*, 1–46 and references therein.

(19) (a) Winkler, H. J. S.; Winkler, H. *J. Am. Chem. Soc.* **1966**, *88*, 964–969. (b) Winkler, H. J. S.; Winkler, H. *J. Am. Chem. Soc.* **1966**, *88*, 969–974. (c) Rogers, H. R.; Houk, J. *J. Am. Chem. Soc.* **1982**, *104*, 522–525.

(20) Beak, P.; Allen D. J. *J. Am. Chem. Soc.* **1992**, *114*, 3420–3425.

(21) (a) Harada, T.; Katsuhira, T.; Hattori, K.; Oku, A. *J. Org. Chem.* **1992**, *57*, 5805–5807. (b) Harada, T.; Katsuhira, T.; Hattori, K.; Oku, A. *Tetrahedron* **1994**, *50*, 7987–8002.

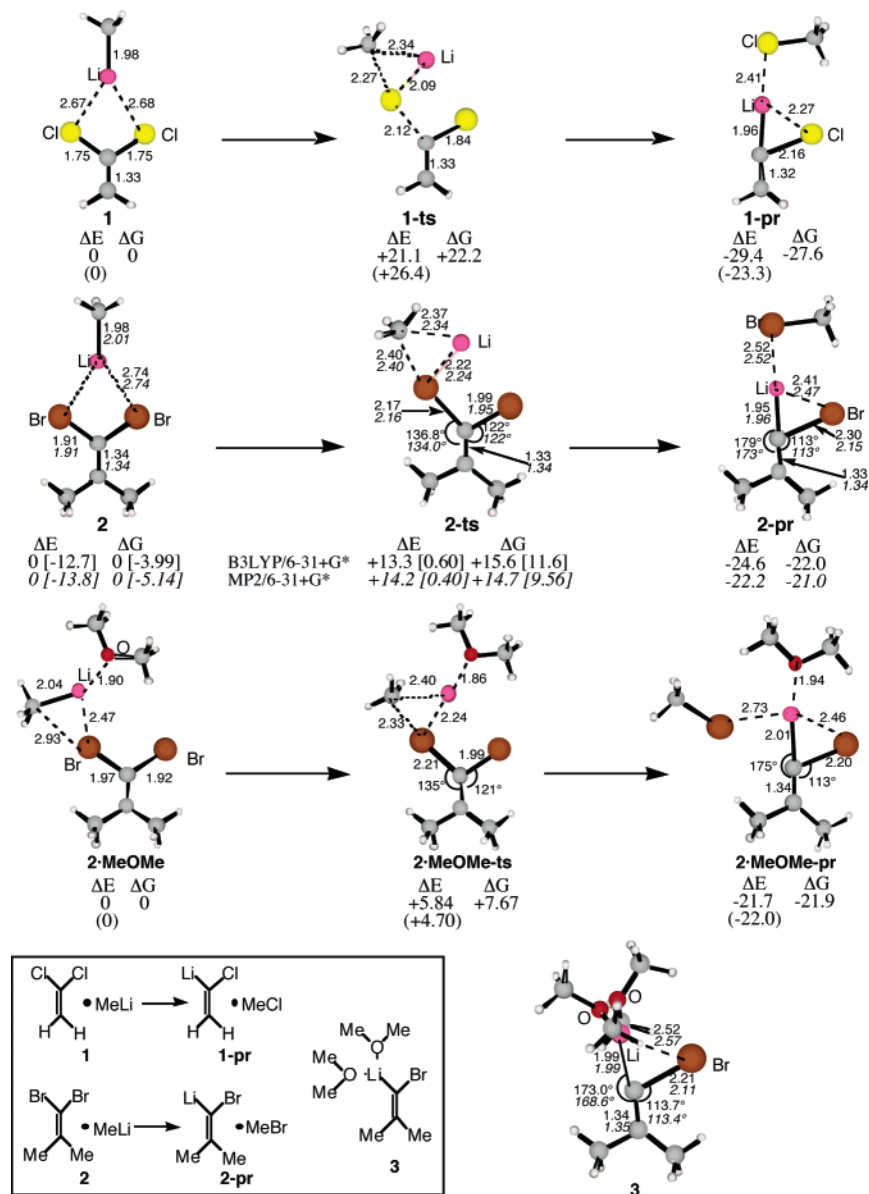


**FIGURE 1.** Transition structures for the lithium–halogen exchange reaction (B3LYP/6-31+G\*).  $\Delta E$  and  $\Delta G$  are the relative energies and the Gibbs free energies at 298.15 K, respectively (kcal/mol). The italic values are the values at the MP2/6-31+G\* level and the values in parentheses are the values of MP2/6-31+G\*/B3LYP/6-31+G\*. The values in square brackets are the energies based on the total energy of CMe<sub>2</sub>=CBr<sub>2</sub> and MeLi.

frequency for all transition structures and confirmed that those structures are authentic transition structures. Starting from the transition state structures, the reaction paths were followed by the IRC analysis.<sup>25</sup> The structures of the reactants, products, and intermediates were obtained from the optimization of the last structures on both sides of the IRC calculations. The

frequency calculations on their structures gave only harmonic frequencies and confirmed that they are minima. Some calculations were performed at the Møller–Plesset second-order perturbation theory (MP2)<sup>26</sup> with the 6-31+G\* basis set. The Gibbs free energies include the corresponding zero-point energies scaled by 0.9670 (reported for MP2/6-31G\*).<sup>24b</sup>

## Results and Discussion

**The Formations of the  $\alpha$ -Halo Alkenyllithium Compounds and Their Structures.** The lithium–halogen exchange reaction of 1,1-dihaloalkenes with methyllithium and the structures of the resulting  $\alpha$ -halo alkenyllithium were first studied (Figure 1). The transition state structure for the lithium–chlorine exchange reaction of 1,1-dichloroethene with methyllithium was located at the B3LYP/6-31+G\* level. The attack by methyllithium on 1,1-dichloroethene initially involves the formation of a loose complex **1** in which the incoming methyllithium is

(22) Frisch, M. J.; Trucks, G. W.; Schlegel, H. B.; Scuseria, G. E.; Robb, M. A.; Cheeseman, J. R.; Zakrzewski, V. G.; Montgomery, J. A., Jr.; Stratmann, R. E.; Burant, J. C.; Dapprich, S.; Millam, J. M.; Daniels, A. D.; Kudin, K. N.; Strain, M. C.; Farkas, O.; Tomasi, J.; Barone, V.; Cossi, M.; Cammi, R.; Mennucci, B.; Pomelli, C.; Adamo, C.; Clifford, S.; Ochterski, J.; Petersson, G. A.; Ayala, P. Y.; Cui, Q.; Morokuma, K.; Malick, D. K.; Rabuck, A. D.; Raghavachari, K.; Foresman, J. B.; Cioslowski, J.; Ortiz, J. V.; Stefanov, B. B.; Liu, G.; Liashenko, A.; Piskorz, P.; Komaromi, I.; Gomperts, R.; Martin, R. L.; Fox, D. J.; Keith, T.; Al-Laham, M. A.; Peng, C. Y.; Nanayakkara, A.; Gonzalez, C.; Challacombe, M.; Gill, P. M. W.; Johnson, B. G.; Chen, W.; Wong, M. W.; Andres, J. L.; Head-Gordon, M.; Replogle, E. S.; Pople, J. A. *Gaussian 98*, revision A.9; Gaussian, Inc.: Pittsburgh, PA, 1998.

coordinated with two chlorine atoms in the plane of the ethene. The transition structure can be seen as either a three-center reaction or the  $S_N2$  mechanism. The activation free energy of the lithium–chlorine exchange reaction is 22.2 kcal/mol. The reaction gives the  $\alpha$ -chloro ethenyllithium compound **1-pr**, where the  $sp^2$  carbon contains both the positive metal (lithium) and the negative leaving group (chlorine) and the C–Cl bond is bridged by the lithium atom. The C–Cl bond in **1-pr** is 0.42 Å longer than that in 1,1-dichloroethene (1.74 Å). The  $^{13}C$  NMR study<sup>2,3</sup> of the  $\alpha$ -bromo alkyllithium compounds showed considerable weakening of the C–Br bonds and the theoretical studies reported a bridging geometry for  $H_2ClLiCl$ ,<sup>4</sup>  $CH_2=CXLi$ ,<sup>5b,13</sup> and  $Me_2C=CCIMgCl$ .<sup>27</sup> The structure **1-pr** is consistent with these previous results. The lithium–bromine exchange reaction of the 1,1-dibromo-2-methylpropene with methyllithium occurred in a similar manner as the lithium–chlorine exchange reaction. The transition structure **2-ts** is similar to **1-ts** and the activation energy is lower than that by 6.6 kcal/mol. The resulting product is the  $\alpha$ -bromo alkenyllithium compound **2-pr**, where the C–Br bond is bridged by the lithium atom. The C–Br bond in **2-pr** is 0.40 Å longer than that in 1,1-dibromo-2-methylpropene (1.90 Å).

Since the above activation energies of the lithium–halogen exchange reaction were higher than we had expected, we further located the transition structure for **2** in the presence of one dimethyl ether molecule (**2-MeOMe-ts**). Since the lithium–halogen exchange reaction is generally performed in THF and dimethyl ether has about the same basicity and steric effect as THF but significantly smaller for computations,<sup>28,29</sup> dimethyl ether was used as coordinating solvent instead of THF. The activation energy is now 7.67 kcal/mol (7.9 kcal/mol lower than that in the gas phase) and this lithium–bromine exchange reaction is an easy process. Furthermore, the structure **3** of 1-bromo-1-lithium-2-methylpropene in the presence of two dimethyl ether molecules was optimized. The C–Br bond is 0.09 Å shorter than that in **2-pr**, while the Li–C and Li–Br distances are 0.04 and 0.11 Å longer than that in **2-pr**, respectively. In the presence of coordinating solvent, the C–Br bond is strengthened. A similar solvent effect was reported by Pratt et al.<sup>5</sup> They studied both monomers and dimers of chloromethylithium and  $CH_2=CXLi$  (X = Cl, Br) in the gas phase and in dimethyl ether or THF solvent by DFT calculations and concluded that those carbenoids exist mainly as monomers in ethereal solvents.

For comparison, the transition structure of the lithium–bromine exchange reaction of **2** was reoptimized at the MP2/6-31+G\* level of theory. Since the MP2 structures of **2** and **2-ts** are similar to the B3LYP ones (compare the bond lengths and the angles in **2** and **2-ts**), the MP2 energies for the other transition structures were calculated with the B3LYP geometries

and the results are shown in Figure 1. The MP2 energies were also not so different from the B3LYP ones. However, the MP2 structure of **2-pr** is a little different from the B3LYP one. The C–Br bond is 0.15 Å shorter, the Li–Br distance is 0.06 Å longer, and the angle C=C–Li is smaller by 6°. Thus, the C–Br bond is strengthened at the MP2 level. We also reoptimized the structure **3** containing two dimethyl ether molecules at the MP2 level to see the structure of  $\alpha$ -bromo alkenyllithium in THF solvent. The C–Br bond is 0.10 Å shorter, the Li–Br distance is 0.05 Å longer, and the angle C=C–Li is smaller by 4.4° than the B3LYP structure (see the italic numbers in **3**). The energies were computed with a higher level of correlation method, a coupled-cluster theory (CCSD(T))<sup>30</sup> with the 6-31+G\* basis set on both the B3LYP and the MP2 structures. The energy difference is only 0.04 kcal/mol, favorable to the B3LYP structure.

It is well-known that alkyllithium compounds exist as aggregate forms in solution. For example, both  $^1H$  and  $^6Li$  NMR spectra show that methyllithium exists primarily as tetrameric and dimeric aggregates in THF.<sup>31,32</sup> To know how the reaction occurs with the aggregate forms of alkyllithium, the transition structure for the lithium–bromine exchange reaction of 1,1-dibromo-2-methylpropene with methyllithium dimer was further located at the MP2 level of theory with the 6-31+G\* basis set (Figure 2). The insertion of one of the bromine atoms to the Me–Li bond in the complex **4** occurs with 9.69 kcal/mol activation energy and the intermediate **4-int1** forms. The intermediate **4-int1** can be seen as either a mixed aggregate form or a bromine ate complex, from which the nucleophilic attack of methyl anion on the bromine atom induced the formation of the mixed aggregate **4-pr** composed of  $\alpha$ -halo alkenyllithium, methyllithium, and bromomethane. The rate-limiting step is the first transition state **4-ts1** and the activation energy is lower than the reaction with the monomer (**2-ts**). The results at the B3LYP/6-31+G\* level are also shown in Figure 2. Although the structures of both **4** and **4-ts1** are about the same as the ones at the MP2 level, the IRC calculation from **4-ts1** gave an intermediate **4-int1'**, which led to **4-int1** via the methyl anion rotation **4-ts1'**. The B3LYP geometries are also very close to the MP2 ones for **4-int1**, **4-ts2**, and **4-pr**. Since the barrier of the methyl rotation **4-ts1'** is only 0.02 kcal/mol ( $\Delta E$ ), the B3LYP results are essentially the same as the MP2 results. Judging from both the activation energies based on  $CMe_2=CBr_2$  and [MeLi or MeLi dimer] (9.56 kcal/mol for **2-ts** vs 8.90 kcal/mol for **4-ts1** at the MP2 level) and the stability of the dimeric MeLi compared with the monomer, the lithium–bromine exchange reaction seems to proceed via dimeric methyllithium. Furthermore, we studied the lithium–bromine exchange reaction of 1,1-dibromo-2-methylpropene with the tetrahedral tetramer of methyllithium. After many trials, we could not locate any transition structures with the tetrahedral tetramer of methyllithium. In general, dimeric aggregates are much more reactive than tetrameric ones. The higher reactivity of the dimer compared with the higher aggregates can be attributed to less steric hindrance and more negative charge density on alkyl groups.

We turned our attention to the stereochemistry of the halogen–lithium exchange reaction of dihaloalkene with alkyl-

(23) (a) Becke, A. D. *J. Chem. Phys.* **1993**, *98*, 5648–5652. (b) Lee, C.; Yang, W.; Parr, R. G. *Phys. Rev. B* **1988**, *37*, 785–789.

(24) (a) Bauschlicher, C. W., Jr.; Partridge, H. *J. Chem. Phys.* **1995**, *103*, 1788–1791. (b) Scott, A. P.; Radom, L. *J. Phys. Chem.* **1996**, *100*, 16502–16513.

(25) (a) Gonzalez, C.; Schlegel, H. B. *J. Phys. Chem.* **1989**, *90*, 2154–2161. (b) Gonzalez, C.; Schlegel, H. B. *J. Phys. Chem.* **1990**, *94*, 5523–5527.

(26) Møller, C.; Plesset, M. S. *Phys. Rev.* **1934**, *46*, 618–622.

(27) Satoh, T.; Ogino, Y.; Ando, K. *Tetrahedron* **2005**, *61*, 10262–10276.

(28) (a) Abbot, A.; Streitwieser, A.; Schleyer, P. v. R. *J. Am. Chem. Soc.* **1997**, *119*, 11255–11268. (b) Ando, K. *J. Org. Chem.* **1999**, *64*, 6815–6821. (c) Pratt, L. M.; Streitwieser, A. *J. Org. Chem.* **2003**, *68*, 2830–2838.

(29) For the use of THF as a coordinating solvent, see: Pratt, L. M. *Bull. Chem. Soc. Jpn.* **2005**, *78*, 890–898.

(30) Pople, J. A.; Head-Gordon, M. *J. Chem. Phys.* **1987**, *87*, 5968–5975.

(31) Corruble, A.; Davoust, D.; Desjardins, S.; Fressigne, C.; Giessner-Prettre, C.; Harrison-Marchand, A.; Houte, H.; Lasne, M.-C.; Maddaluno, J.; Oulyadi, H.; Valnot, J.-Y. *J. Am. Chem. Soc.* **2002**, *124*, 15267–15279.

(32) Schleyer, P. v. R. *Pure Appl. Chem.* **1984**, *56*, 151–162 and references therein.



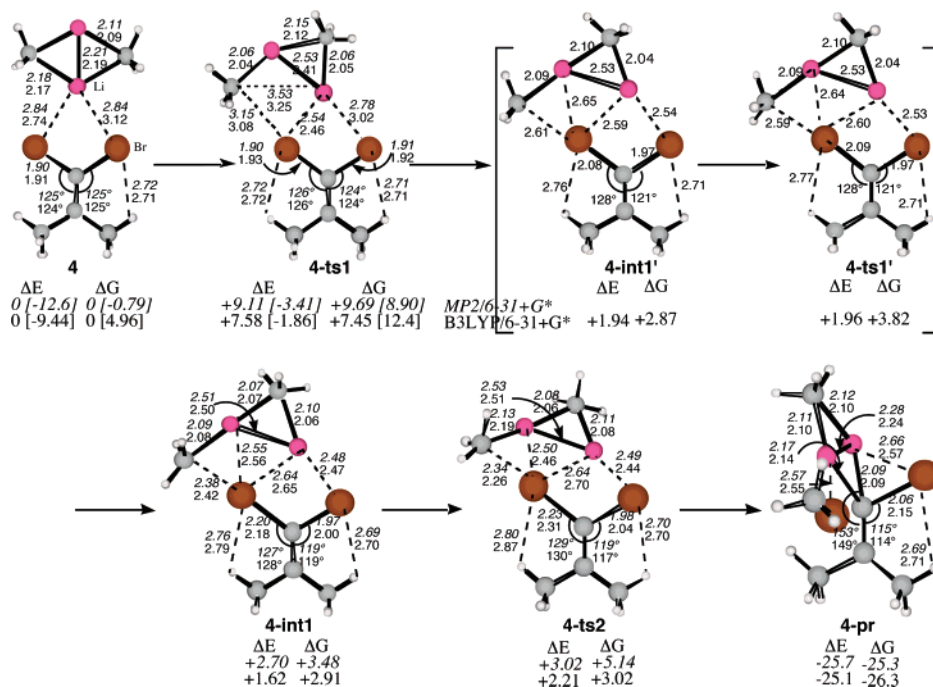
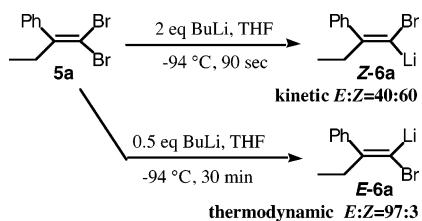


**FIGURE 2.** Transition structures for the lithium–halogen exchange reaction of dibromoolefin with methyl lithium dimer (MP2/6-31+G\*) (italic numbers). The values of the B3LYP/6-31+G\* results are also shown.  $\Delta E$  and  $\Delta G$  are the relative energies and the Gibbs free energies at 298.15 K, respectively (kcal/mol). The values in square brackets are the energies based on the total energy of CMe<sub>2</sub>=CBr<sub>2</sub> and MeLi dimer.

#### SCHEME 2



lithium. The stereochemistry of the lithium–bromine exchange reaction of 1,1-dibromoalkenes with alkyllithium was experimentally studied.<sup>21,33</sup> The lithium carbenoids derived from 1,1-dibromoalkenes are configurationally stable at low temperature (−94 °C), whereas, in the presence of the unreacted dibromoalkenes, the lithium carbenoids undergo facile isomerization. When a THF solution of dibromoalkene **5a** was added to a THF–hexane solution of BuLi (2 equiv) at −94 °C during a 90-s period, a 40:60 mixture of lithium carbenoids *E*- and *Z*-**6a** was obtained (kinetic condition) (the ratio was determined after the treatment with AcOH/THF) (Scheme 2).<sup>21b</sup> Addition of BuLi to a solution of **5a** (2 equiv) during a 90-s period followed by standing the resulting mixture for 30 min at −94 °C gave a 97:3 mixture of *E*- and *Z*-**6a** (thermodynamic condition). The kinetically controlled attack on the sterically more hindered bromine atom is noteworthy. To see whether our model system can predict the stereochemistry correctly, we located the transition structures of the lithium–bromine exchange reaction of 1,1-dibromoalkenes **5a** with MeLi at the B3LYP/6-31+G\*

level. The results are shown in Figure 3. The product ratios were calculated from the equation  $k_1/k_2 = e^{-\Delta\Delta E(\text{calcd})/RT}$  or  $e^{-\Delta\Delta G(\text{calcd})/RT}$ , where  $\Delta\Delta E$  and  $\Delta\Delta G$  are the differences between the energies and the Gibbs free energies calculated for the two transition structures or two products at −94 °C, respectively. The calculated Gibbs free energy difference between *E*-**5a-ts** and *Z*-**5a-ts** ( $\Delta\Delta G = 0.32$  kcal/mol) corresponds to the product ratio of 29:71 (kinetic), and the calculated product energy difference ( $\Delta\Delta G = 1.03$  kcal/mol) corresponds to 95:5 (thermodynamic) at −94 °C. These predictions are in good agreement with experimental results. The distance between the ethyl-H and the bromine in **5a-MeLi** is 2.73 Å, which is less than the sum of their van der Waals radii (3.05 Å). Since the C–C–Br angle expands to 137° in *Z*-**5a-ts**, the steric repulsion diminishes, while the expansion of the other C–C–Br angle in *E*-**5a-ts** causes the rotation of the phenyl ring and more overlap of  $\pi$ -bonds stabilizes the transition structure. Therefore, *Z*-**5a-ts** is only slightly more stable than *E*-**5a-ts**. The single point energy calculations at the MP2/6-31+G\* level were performed on the B3LYP structures *E*-**5a-ts** and *Z*-**5a-ts**. Since the energy difference was 0.85 kcal/mol and much bigger than the value (0.15 kcal/mol) calculated from the experimental selectivity, the transition structures were also located at the MP2/6-31+G\* level. The MP2 geometries are similar to the B3LYP ones with the angles C=C–Br(replaced) smaller by 2.5–5.1°. The calculated energy difference between *E*-**5a-ts** and *Z*-**5a-ts** ( $\Delta\Delta G = 0.23$  kcal/mol) corresponds to the product ratio of 34:66 [exptl(kinetic), 40:60] and the calculated product energy difference ( $\Delta\Delta G = 1.15$  kcal/mol) corresponds to 96:4 [exptl(thermodynamic), 97:3] at −94 °C. These calculations predict the product selectivity in both the kinetic and the thermodynamic conditions extremely well. The bigger angles C=C–Br(replaced) in the B3LYP structures make the calculated energy difference between *E*-**5a-ts** and *Z*-**5a-ts** greater.

The transition structures for the lithium–bromine exchange

(33) (a) Mahler, H.; Braun, M. *Tetrahedron Lett.* **1987**, 28, 5145–5148. (b) Barluenga, J.; Rodríguez, M. A.; Campos, P. J.; Asensio, G. *J. Am. Chem. Soc.* **1988**, 110, 5567–5568. (c) Rayner, C. M.; Astles, P. C.; Paquette, L. A. *J. Am. Chem. Soc.* **1992**, 114, 3926–3936. (d) Grandjean, D.; Pale, P. *Tetrahedron Lett.* **1993**, 34, 1155–1158. (e) Braun, M.; Rahematpura, J.; Böhne, C.; Paulitz, T. C. *Synlett* **2000**, 1070–1072. (f) Li, Y.; Lu, L.; Zhao, X. *Org. Lett.* **2004**, 6, 4467–4470.

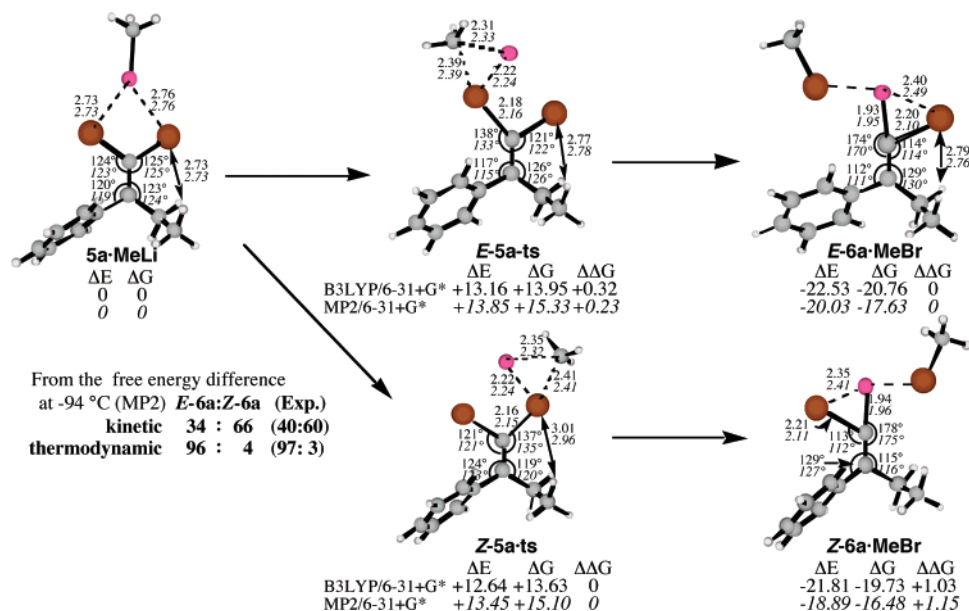


**FIGURE 3.** Transition structures for the lithium–halogen exchange reaction of the dibromoalkene **5a** with MeLi [B3LYP/6-31+G\*].  $\Delta E$  and  $\Delta G$  are the relative energies and the Gibbs free energies at  $-94$  °C, respectively (kcal/mol).  $\Delta\Delta G$  is the free energy difference between the *E* and *Z* series. The italic values are the values at the MP2/6-31+G\* level.

**TABLE 1.** Stereochemistry of the Lithium–Bromine Exchange Reaction under Both Kinetic and Thermodynamic Conditions (B3LYP/6-31+G\*)

substrate	temp, °C	exptl <sup>12b</sup> <i>E:Z</i>	calculated	
			<i>E:Z</i> ( $\Delta\Delta G$ of <i>E1:E2:Z1:Z2</i> )	<i>E:Z</i> ( $\Delta\Delta E$ of <i>E1:E2:Z1:Z2</i> )
<b>5a</b>	-94	product ratio ( <i>E:Z</i> ) under the kinetic condition 40:60	29:71 (0.32:0)	19:81 (0.52:0) 8:92 (0.85:0) <sup>a</sup>
			34:66 (0.23:0) <sup>b</sup>	24:76 (0.41:0) <sup>b</sup>
<b>5b</b>	-116	19:81	3:97 (1.11:2.86:0:1.15)	2:98 (1.27:2.86:0:1.78)
<b>5c</b>	-94	71:29	88:12 (0:4.23:0.72:4.62)	95:5 (0:3.41:1.03:4.06)
<b>5a</b>	-94	product ratio ( <i>E:Z</i> ) under the thermodynamic condition 97:3	95:5 (0:1.03)	88:12 (0:0.72) 93:7 (0:0.90) <sup>a</sup>
			96:4 (0:1.15) <sup>b</sup>	96:4 (0:1.14) <sup>b</sup>
<b>5b</b>	-116	24:76	45:55 (0.05:2.03:0:0.89)	25:75 (0.35:1.75:0:1.09)
<b>5c</b>	-94	99:1	89:11 (0:2.34:0.76:5.69)	87:13 (0:1.76:0.69:4.89)

<sup>a</sup> The energies at the MP2/6-31+G\*/B3LYP/6-31+G\* level. <sup>b</sup> The energies at the MP2/6-31+G\* level.

reaction of the dibromoalkenes **5b** and **5c** were located at the B3LYP/6-31+G\* level and the energies are summarized in Table 1 along with the experimental results. Both the reactions of **5b** and **5c** have four transition structures, which are shown together with the products in Figure 4. The energies at the MP2/6-31+G\*/B3LYP/6-31+G\* level were also shown in parentheses in Figure 4. Because of the sterically demanding isopropyl group, the torsional angles between the phenyl and the alkenyl group are  $89.7$ – $90.7^\circ$  in *E,Z-5b-ts1*. Only the steric repulsion between the isopropyl-H and the bromine determines the selectivity. Thus, *Z-5b-ts1* is favored over *E-5b-ts1* by 1.11 kcal/mol. The other two transition structures *E,Z-5b-ts2* derived from the other starting complex **5b'-MeLi** suffer from a big steric repulsion between the two methyl groups and the bromine, and have higher energies than *Z-5b-ts1*. Because of the higher steric repulsion of the bromine with the 1,3-dioxa-2-yl group rather

than the methyl group (see the starting complex **5c-MeLi**), *E-5c-ts1* is favored over *Z-5c-ts1* by 0.72 kcal/mol. The shorter distance from the vinyl-Br to the 1,3-dioxa-2-yl-H rather than to the methyl-H in **5c-MeLi** was caused by a smaller angle for the C=C–C ( $120^\circ$ ). To know why this angle is smaller than the other ( $124^\circ$ ), we optimized the MeLi complex of 1,1-dibromo-2,3-dimethylbut-1-ene (**5d-MeLi**). Due to the sterically crowded isopropyl group, the angle C–C–H decreases from the tetrahedral to  $108^\circ$ ; on the other hand, the angle C–C–H on the methyl side increases to  $113^\circ$  in order to reduce the steric repulsion with the bromine atom. Thus, the isopropyl group has a larger steric hindrance than the methyl group in **5d-MeLi**. However, the difference of the C–C–H angles in **5c-MeLi** is small. Since an oxygen atom has a smaller space than a methyl group, steric crowding is not very important here. Rather than that, the electrostatic repulsion between the olefin  $\pi$ -electron

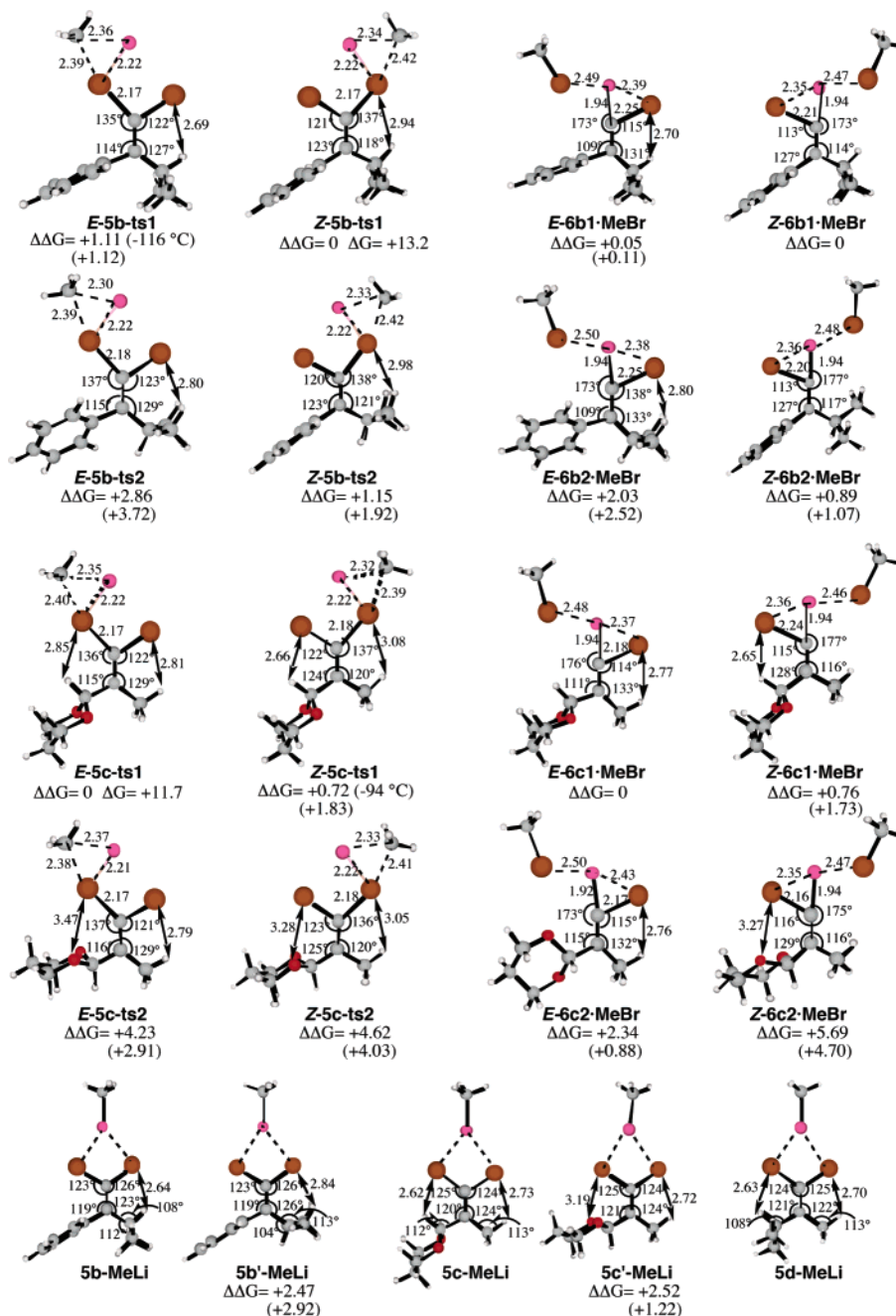


**FIGURE 4.** Transition structures for the lithium–halogen exchange reaction of the dibromoalkenes **5b** and **5c** with MeLi [B3LYP/6-31+G\*]. Products **6b** and **6c** and the starting complexes **5b-MeLi**, **5c-MeLi**, and **5d-MeLi** are also shown.  $\Delta\Delta G$  and  $\Delta G$  are the Gibbs free energy difference and the activation free energy at  $-116$  °C for **5b** and **6b** and  $-94$  °C for **5c** and **6c** (kcal/mol), respectively. The values in parentheses are the energies at the MP2/6-31+G\*/B3LYP/6-31+G\* level.

and the oxygen lone pair seems important.<sup>34</sup> If the C=C–C angle expands in **5c-MeLi** to reduce the steric repulsion with the bromine atom, the electrostatic repulsion increases. Thus, the 1,3-dioxa-2-yl group has a larger steric hindrance than the methyl group in **5c-MeLi**. Both the transition structures *E*,*Z*-**5c-ts2** derived from the other dibromoalkene conformer **5c'-MeLi** are more than 4 kcal/mol less stable than *E*-**5c-ts1** due to the electrostatic repulsion between the two oxygen atoms and the bromine atom. In all cases, the sterically more constrained bromine atoms of 1,1-dibromoalkenes were predominantly

reacted with alkyllithium in the kinetic condition. Although the energy differences at the B3LYP level were a little larger because of the bigger C=C–Br(replaced) angles, the product ratios calculated from Boltzmann distributions including all transition structures are in good agreement with the experimental results.

The product *Z*-**6b1-MeBr** is slightly more stable than *E*-**6b1-MeBr**. The steric repulsion between the alkyl group and the bromine atom is expected for *E*-**6b1-MeBr**, whereas the electrostatic repulsion between the bromine lone pairs and the phenyl  $\pi$ -electrons destabilizes *Z*-**6b1-MeBr**. Therefore, the energy difference is small and the experimental selectivity in the thermodynamic condition is lower than that in the kinetic

(34) Ando, K. *J. Am. Chem. Soc.* **2005**, *127*, 3964–3972.

(35) Barone, V.; Cossi, M. *J. Phys. Chem. A* **1998**, *102*, 1995–2001.

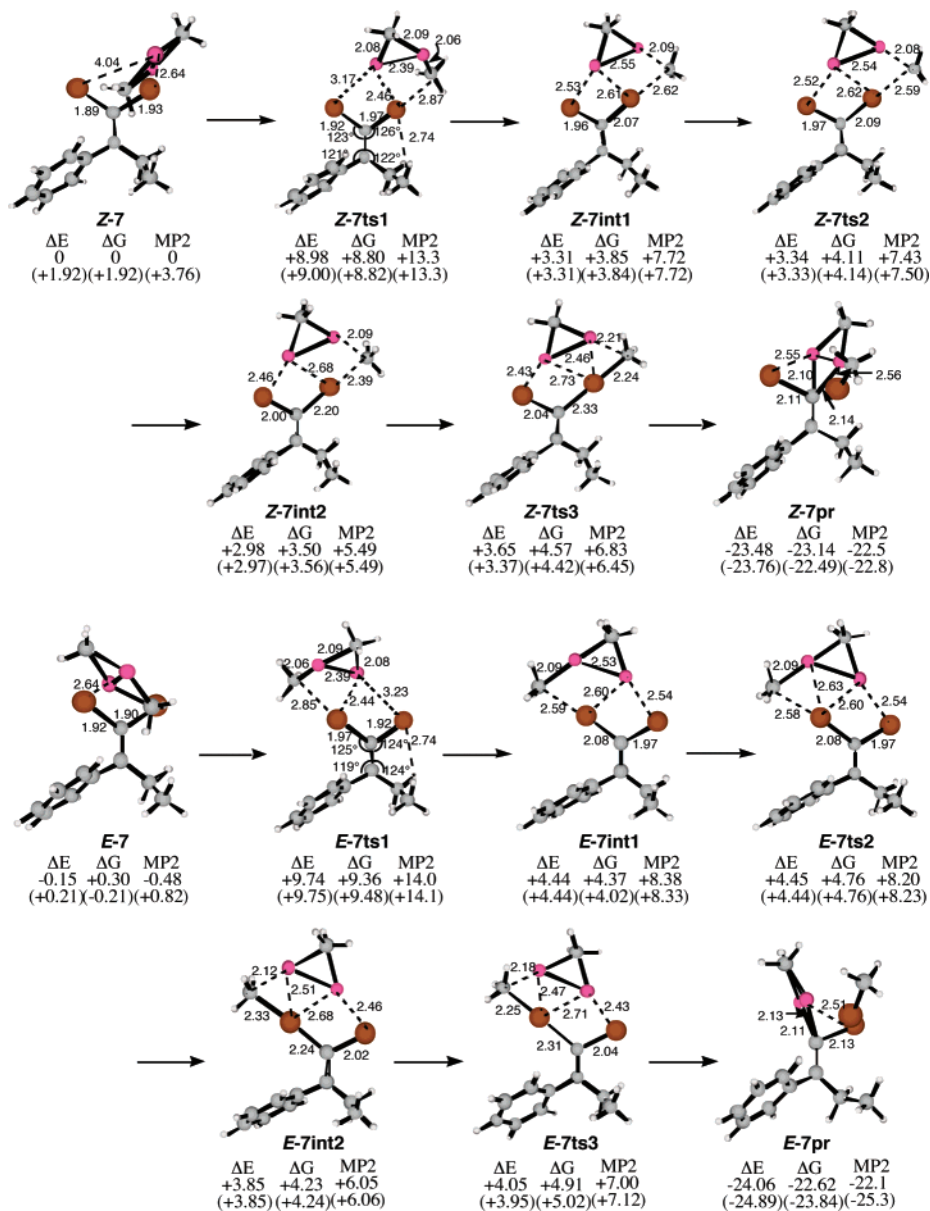


**FIGURE 5.** Transition structures for the lithium–halogen exchange reaction of the dibromoalkenes **5a** with MeLi dimer [B3LYP/6-31+G\*].  $\Delta E$  and  $\Delta G$  are the relative energies and the Gibbs free energies at  $-94^\circ\text{C}$ , respectively (kcal/mol). MP2 is the relative energy at the MP2/6-31+G\*\*/B3LYP/6-31+G\* level. The numbers in parentheses are the relative energies of the other structures with the Me group retreating into the page.

condition. Comparing these structures with **6a-MeBr**, **E-6a-MeBr** is less sterically crowded than **E-6b1-MeBr** and is stabilized by more overlap of  $\pi$ -bonds. Consequently, **E-6a-MeBr** is favored over **Z-6a-MeBr** by 1.03 kcal/mol. Since **E,Z-6c1-MeBr** have two alkyl groups on one of the double bond carbons and only steric repulsion determines the product stability, **E-6c1-MeBr** is favored over **Z-6c1-MeBr** by 0.76 kcal/mol. The energy differences of these product conformers are in good agreement with the product ratios in the thermodynamic condition as shown in Table 1.

The transition structures of the lithium–bromine exchange reaction of 1,1-dibromoalkenes **5a** with dimeric methyllithium were also located at the B3LYP/6-31+G\* level and the four types of the reaction paths are obtained. The energies were also calculated at the MP2/6-31+G\*\*/B3LYP/6-31+G\* level. Two of them are shown in Figure 5, together with the energies of the other two paths. Although the structures of the starting complexes **E,Z-7** are different from that of **4** in Figure 2, the

transition structures, the intermediates, and the products are almost the same as the structures in Figure 2. The corresponding coplaner complex for **5a** with the dimeric methyllithium is 1.92 kcal/mol less stable than **Z-7**. The reaction occurs with the formation of the bromine ate complex, followed by methyl anion rotation, and the nucleophilic attack of methyl anion on the bromine atom. The rate-limiting step is the formation of the bromine ate complex, **7ts1**. The transition structure **Z-7ts1** is 0.56 kcal/mol more favorable than **E-7ts1**. This energy difference ( $\Delta\Delta G = 0.56$  kcal/mol) corresponds to  $E:Z = 17:83$  (exptl 40:60) at  $-94^\circ\text{C}$ . The product **E-7pr** (not shown) is more stable than **Z-7pr** by 0.70 kcal/mol. This difference corresponds to  $E:Z = 88:12$  (exptl 97:3). These calculations predict the selectivity of the product correctly.

For the intramolecular substitution reaction shown in eq 3, the reaction of lithium 4,4-dibromo-3-methyl-3-pentenoate with methyllithium (**8**) was chosen as a model system (Figure 6). The lithium–bromine exchange reaction of **8** was studied at



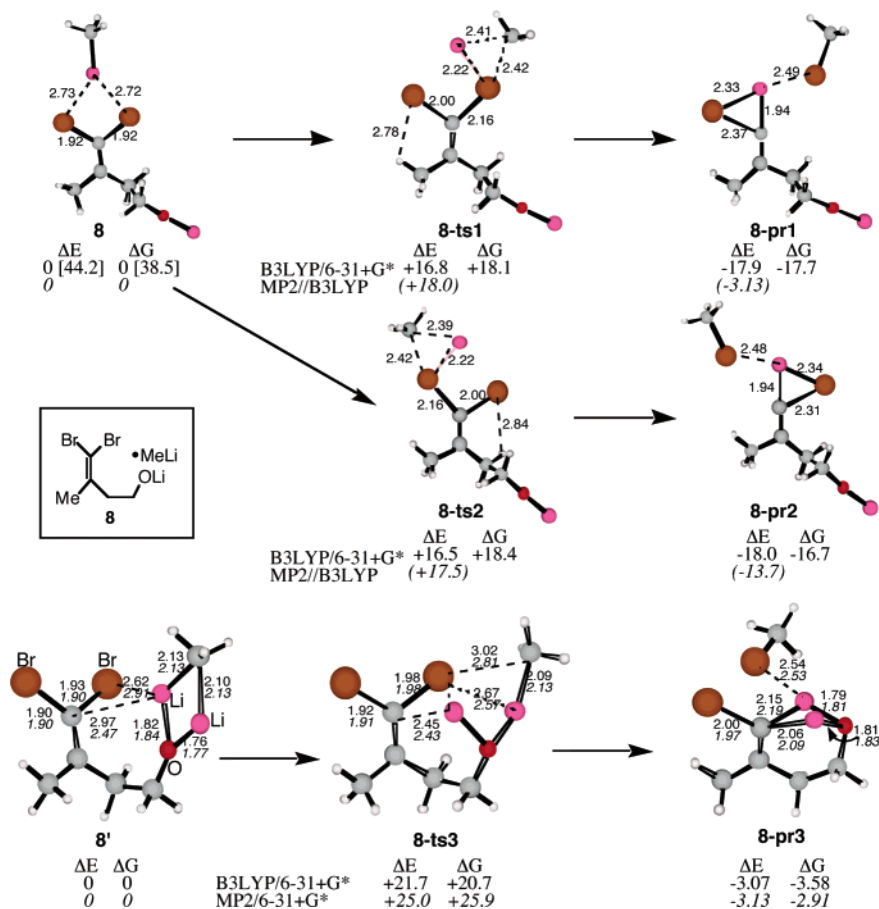
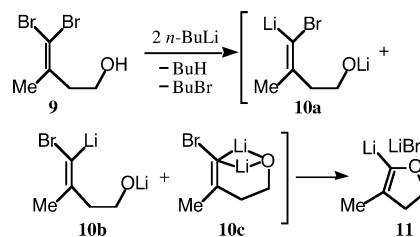


**FIGURE 6.** Transition structures for the lithium–bromine exchange reaction (B3LYP/6-31+G\*).  $\Delta E$  and  $\Delta G$  are the differences in energy and the Gibbs free energy at 298.15 K, respectively (kcal/mol). The italic values are the values at the MP2/6-31+G\* level and the values in parentheses are the values of MP2/6-31+G\*//B3LYP/6-31+G\*. The values in the square brackets under **8** are the relative energies based on those of **8'**. The numbers in the structures are bond lengths (Å).

the B3LYP/6-31+G\* level. The activation energy of the lithium–bromine exchange reaction of **8** is 18.1 and 18.4 kcal/mol for the transition structures **8-ts1** and **8-ts2**, respectively. Since both the steric environments of **8-ts1** and **8-ts2** are almost the same, their energies are about the same. The MP2 energies were also not so different from the B3LYP ones. The lithium–bromine exchange reaction can also occur by the attack of the methyl lithium having coordination to the O–Li part of **8**. The transition structures were located at both the B3LYP and the MP2 levels of theory with the 6-31+G\* basis set. The activation free energies for the lithium–bromine exchange reaction of **8'** are 20.7 and 25.9 kcal/mol, respectively, and the resulting lithium compound is **8-pr3**. Although the C–Br bond in **8-pr3** is not bridged by the lithium atom, it is still 0.10 Å longer than that in **8'**. The structure **8-pr3** is rather similar to the crystal structure of 1-chloro-2,2-bis(4-chlorophenyl)-1-lithioethene in the presence of THF and tetramethylethylenediamine (TMEDA) at  $-115\text{ }^\circ\text{C}$ , where the lithium atom is solvated by TMEDA and THF.<sup>6</sup> The activation energy of the lithium–bromine exchange reaction of **8'** is higher than that of **8** by 2.6 kcal/mol, while the structure **8** is less stable than **8'** by 38.5 kcal/mol. Since this reaction was performed in toluene (eq 3), the route from **8'** to **8-pr3** via **8-ts3** is the most plausible for the lithium–bromine exchange reaction. However, the lithium compounds are either aggregated or the lithium cation is solvated in solution. Therefore, the comparison of these two lithium–bromine exchange processes is not straightforward. For example,

the dimer of **8** having the  $-(\text{O}-\text{Li})_2-$  cluster structure is stabilized by 55.9 kcal/mol. That is, the unit **8** is stabilized by 28.0 kcal/mol by taking the dimeric form. Furthermore, the solvation of the lithium cation would stabilize **8** much more than **8'**. The *E* and *Z* isomerization of  $\alpha$ -halo alkenyllithium compounds also occurs even at low temperature.<sup>6</sup> Therefore, we decided to study all of the organolithium species **8-pr1**, **2**, and **3** for the intramolecular substitution reaction.

**The Intramolecular Substitution Reaction of 4,4-Dibromo-3-methyl-3-pentanol on Treatment with *n*-BuLi.** From the above study of the lithium–halogen exchange reaction, the formation of  $\alpha$ -bromo alkenyllithium species **10a–c** was expected on the treatment of **9** with 2 equiv of *n*-BuLi. The structures **10a–c** were obtained by removing methyl bromide from **8-pr1**, **2**, and **3** and optimizing the resultant structures.



The structures **10a** and **10b** are the two isomers where the C–Br bond is bridged by the lithium atom. Although the B3LYP

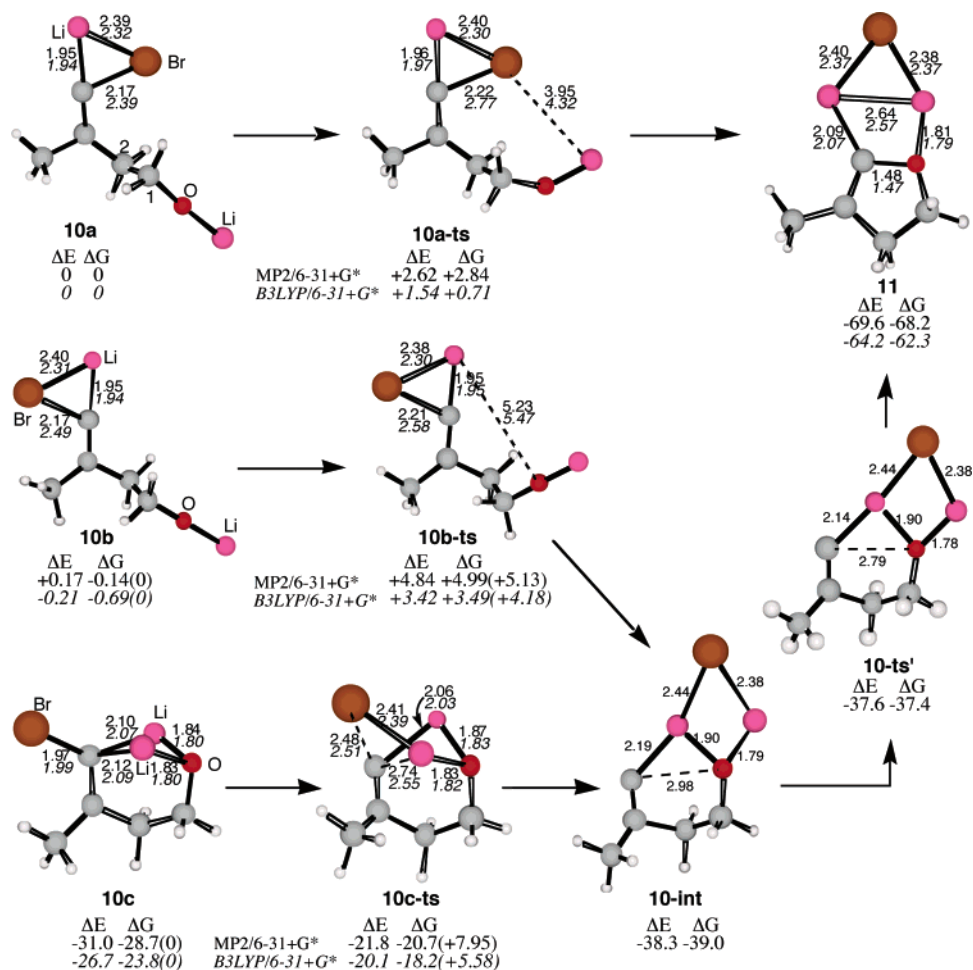


**FIGURE 7.** Transition structures for the intramolecular substitution reaction of  $\alpha$ -bromo alkenyllithium **10** (MP2/6-31+G\*).  $\Delta E$  and  $\Delta G$  are the relative energies based on those of **10a** at 298.15 K (kcal/mol). The italic values are the values at the B3LYP/6-31+G\* level. The numbers in the structures are bond lengths ( $\text{\AA}$ ).

transition structures for the lithium–halogen exchange reactions were very close to the MP2 ones, the structures of the  $\alpha$ -bromo alkenyllithium compounds are a little different from the MP2 ones with the shorter C–Br bond and the longer Li–Br bond. Therefore, the calculations were performed at both the MP2 and the B3LYP levels (Figure 7). The isomer **10b** is more stable than **10a** by 0.14 (B3LYP: 0.69) kcal/mol in Gibbs free energy. The intramolecular substitution reactions of **10a** and **10b** require activation energy of 2.84 (0.71) and 5.13 (4.18) kcal/mol, respectively, to give the dihydrofuran **11**. Both the transition structures **10a-ts** and **10b-ts** are the rotational ones around the C1–C2 bond in essence in both the MP2 and the B3LYP levels. When the O–Li part becomes close enough to the Li–Br part of the molecule, they attract each other and the bromine atom is completely apart from the alkyldene carbon. After that, the C–O bond forms to make the dihydrofuran **11**. The existence of the lithium bridged structure makes **10c** more stable than **10a** by 28.7 (23.8) kcal/mol. The cyclization reaction of **10c** is also an easy process, which requires activation energy of 7.95 (5.58) kcal/mol. Since this cyclization reaction seemed to proceed by the in-plane  $S_N2$ -type mechanism, we performed a full intrinsic reaction coordinate (IRC) analysis of this reaction for deeper understanding of the reaction mechanism. The IRC analysis was carried out at the B3LYP/6-31+G\* level. Several representative intermediates on the IRC are shown together with

those energies in Figure 8. From the starting point of the reactant **10c**, the energy increases with the increase in the distance of the C–Br bond. At the transition state (**10c-ts**), the C–Br bond is almost broken (2.51  $\text{\AA}$ ), while the C–O distance is still not much shorter than that in **10c** (2.74  $\text{\AA}$  vs 2.86  $\text{\AA}$ ). After going beyond the transition state, **10c-ts**, the energy decreases rapidly with the continuous increase in the C–Br distance. In the last structure **A** of the IRC analysis, the distances of C–Br and C–O are 3.52 and 3.12  $\text{\AA}$ , respectively. Optimization starting from **A** gave **11**. The results show that the reaction occurs with the C–Br bond dissociation followed by the C–O bond formation. At the MP2 level, the IRC calculations from both **10b-ts** and **10c-ts** gave the intermediate **10-int**, which led to **11** via **10-ts'**. Since the activation energy of **10-ts'** is only 1.56 kcal/mol, the MP2 results are essentially the same as the B3LYP ones.

In all these mechanisms, the driving force of the reaction is the Li/Br or Li/O interaction rather than the nucleophilic attack by the oxyanion, and the intramolecular substitution reactions of  $\alpha$ -bromo alkenyllithium compounds proceed in a concerted manner. Although the activation energy of the cyclization of **10a** and **10b** is lower than that of **10c**, the structures **10a** and **10b** are much less stable than **10c**. Accordingly, the cyclization seems to proceed mainly through **10c** especially in a less polar solvent such as toluene, which is used in the experiment as a solvent.<sup>16</sup>

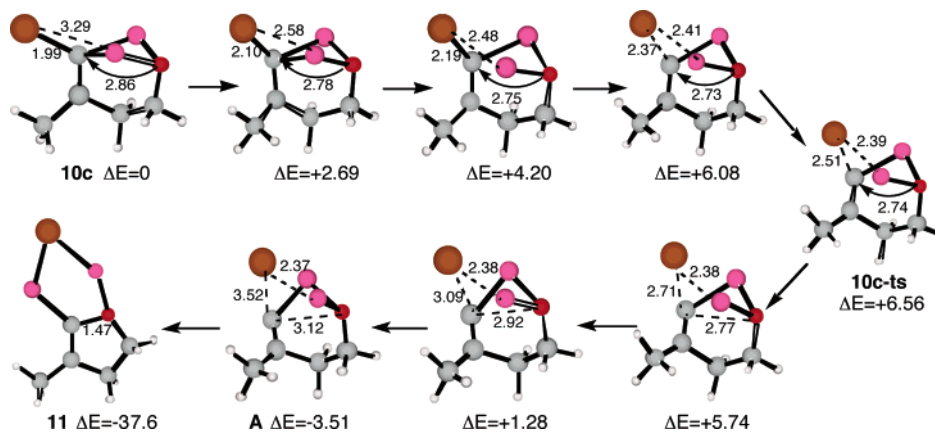


FIGURE 8. Representative intermediates on the IRC of the intramolecular substitution reaction of **10c** [B3LYP/6-31+G\*].

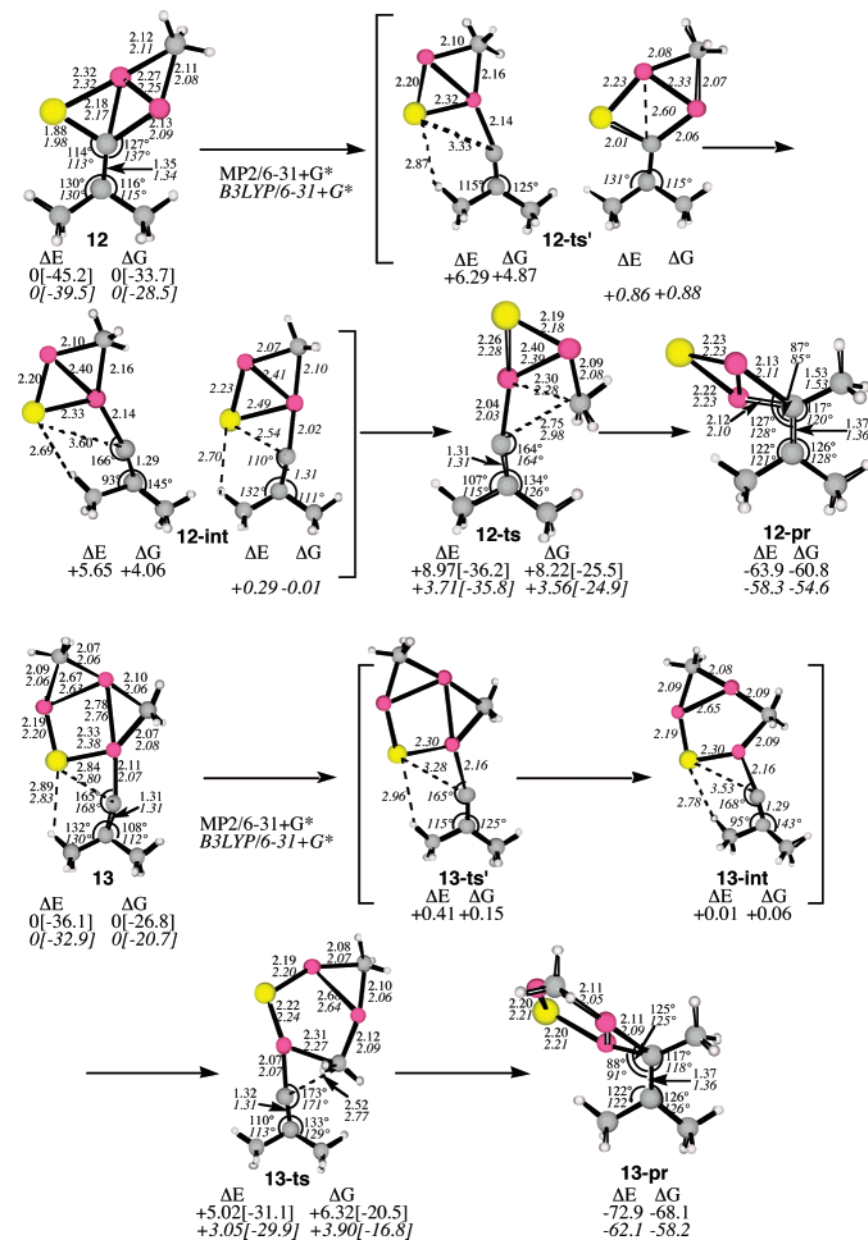
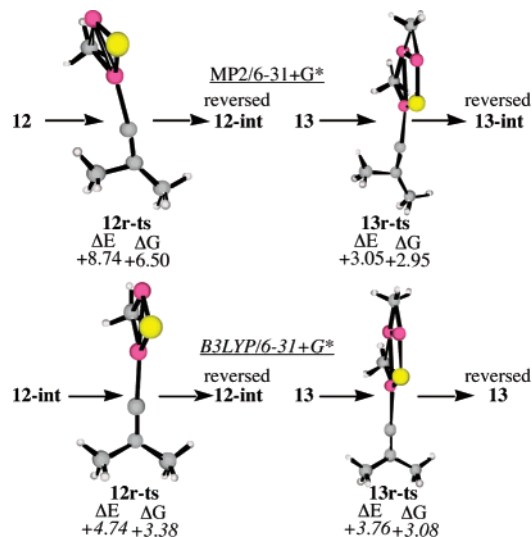


FIGURE 9. Transition structures for the intermolecular substitution reaction of  $\alpha$ -chloro alkenyllithium with MeLi or MeLi dimer (MP2/6-31+G\*).  $\Delta G$  is the relative Gibbs free energy at  $-75^\circ\text{C}$  (kcal/mol). The italic values are the values at the B3LYP/6-31+G\* level. The numbers in the structures are bond lengths ( $\text{\AA}$ ). The values in square brackets are the energies based on the total energy of  $\text{CMe}_2=\text{CLiCl}$  and (MeLi or MeLi dimer).

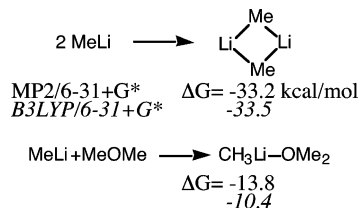


**FIGURE 10.** Transition structures for the isomerization reaction of  $\alpha$ -chloro alkenyllithium complex with MeLi or MeLi dimer [MP2/6-31+G\* and B3LYP/6-31+G\*].  $\Delta G$  is the relative Gibbs free energy at  $-75^\circ\text{C}$ .

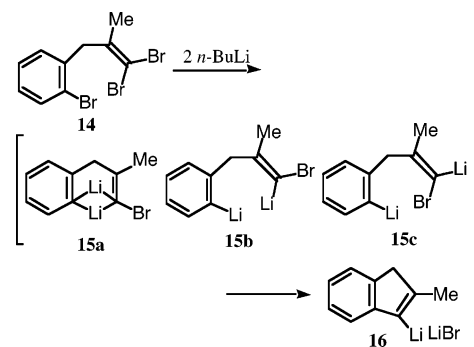
As we mentioned before, inversion of the configuration was reported to a certain extent in the nucleophilic substitution of the optically active  $\alpha$ -chloro alkenyllithium compound (eq 1). To analyze this reaction, we performed a computational study on the nucleophilic substitution of 1-chloro-2-methylpropenyllithium with MeLi (Figure 9). The transition structures were located by the MP2 level of theory with the 6-31+G\* basis set. The bond cleavage of the C–Cl bond in **12** occurs with 4.87 kcal/mol activation energy and the intermediate **12-int** forms. After that, the nucleophilic attack of the methyl anion on the vinyl carbon gave the product **12-pr**. The rate-limiting step is **12-ts** and the activation energy is 8.22 kcal/mol. Although **12-ts** is different from that of the typical  $\text{S}_{\text{N}}2$  reaction, the backside attack of the nucleophile ( $\text{Me}^-$ ) occurs and the stereochemical configuration of the molecule inverts. We further located the transition structure for the isomerization reaction of the complex **12** (Figure 10). The Gibbs free energy of **12r-ts** is 6.50 kcal/mol, which is lower than the energy of **12-ts** by 1.7 kcal/mol. The IRC calculation from **12r-ts** gave the reversed **12-int**. The results at the B3LYP/6-31+G\* level are also shown in Figures 9 and 10. Although both the structures of **12-ts'** and **12-int** and the activation energies are different from the MP2 ones, the reaction essentially proceeds from **12** to **12-pr** via **12-ts**. The activation energy for **12-ts** (3.56 kcal/mol) is about the same as the isomerization energy (3.38 kcal/mol) in Figure 10. Therefore, the stereospecificity is expected to be low.

We also located the transition structures for the nucleophilic substitution reaction of 1-chloro-2-methylpropenyllithium with MeLi dimer (Figure 9). The reaction proceeded in a similar way. That is, the bond cleavage of the C–Cl bond in **13** followed by the nucleophilic attack of the methyl anion on the vinyl carbon gave the product **13-pr**. The rate-limiting step is **13-ts** and the activation energy is 6.32 kcal/mol. However, the activation energy for the isomerization reaction at the MP2 level was quite low (2.95 kcal/mol). In this case, the reaction with MeLi monomer gave a better prediction for the experimental stereospecificity rather than that with the dimer. The activation energies based on the total energy of  $\text{CMe}_2=\text{CHLiCl}$  and (MeLi

or MeLi dimer) are  $-25.5$  and  $-20.5$  kcal/mol for **12-ts** and **13-ts** at the MP2 level, respectively. The dimerization energy for MeLi is 16.6 kcal/mol for one MeLi. If we compare this with the solvation energy for MeLi with dimethyl ether (13.8 kcal/mol), the dimer is 2.8 kcal/mol more stable than the monomer. The activation energy for **12-ts** is lower than that for **13-ts** by 2.2 kcal/mol when this energy difference is added.



**The Intramolecular Substitution Reaction of  $\alpha$ -Bromo Alkenyllithium Compound with Carbon Nucleophile.** The formation of  $\alpha$ -bromo alkenyllithium species, **15a–c** was expected from 3-(*o*-bromophenyl)-1,1-dibromo-1-propene **14** by treatment with 2 equiv of *n*-BuLi. The reaction of these  $\alpha$ -bromo alkenyllithium species with the intramolecular carbon nucleophile was studied at the MP2/6-31+G\* level. The existence of the lithium bridged structure makes **15a** the most stable one. The cyclization reaction of **15a** proceeds in a similar manner as **10c** and gives the cyclization product **16** with the activation energy of 9.90 kcal/mol. The structures **15b** and **15c** are the two isomers where the C–Br bond is bridged by the lithium atom. When the distance between  $\text{Li}_A$  and  $\text{Li}_B$  in **15b** becomes shorter (**15b-ts**), the transformation to **15a** occurs. On the other hand, **15c-int1** is obtained when the distance between Br and  $\text{Li}_B$  in **15c** becomes shorter. The activation energy is only 1.76 kcal/mol. Since the lithium atom interacts with the bromine atom first, the cleavage of the C–Br bond occurs. The cyclization product **16** forms from **15c-int1** via the transition structures **15c-ts2** and **15c-ts3**. After all, all three species give **16** with small activation energies. The results at the B3LYP/6-31+G\* level are similar to the MP2 ones as shown in Figure 11.



No lithium–bromine exchange of the bromophenyl moiety of **14** with *n*-BuLi occurred in toluene, whereas the reaction occurred in THF even at  $-105^\circ\text{C}$ , experimentally.<sup>16</sup> We therefore studied the lithium–bromine exchange reaction of bromobenzene with MeLi (Figure 12). The activation energy for the transition structure **17-ts** is very high (about 35 kcal/mol) and the energy of the product **17-pr** is higher than that of the starting complex **17**. Since the dipole moments of **17** and **17-pr** are 7.95 and 8.78 D (MP2), respectively, the less polar **17** is stabilized in the gas phase. This result is in good agreement with the experimental failure for the lithium–bromine exchange



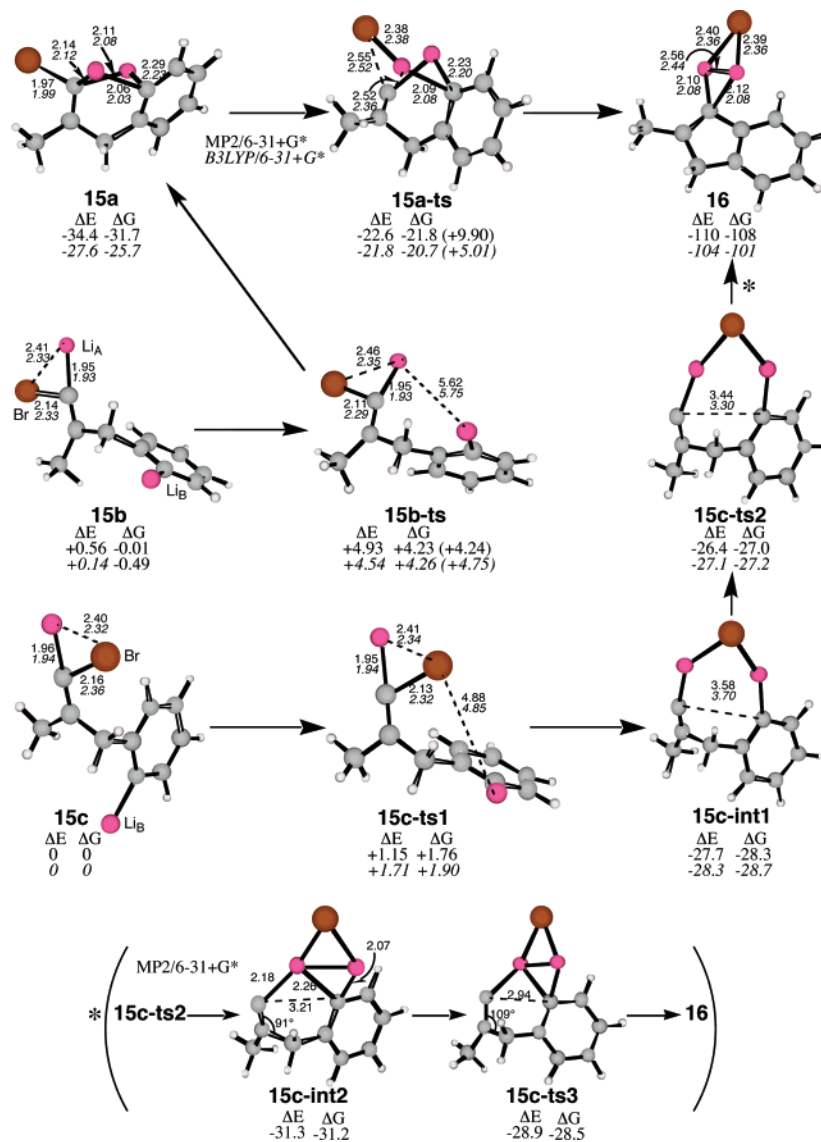


**FIGURE 11.** The reaction paths for the intramolecular reaction of  $\alpha$ -bromo alkenyllithium (MP2/6-31+G\*).  $\Delta G$  is the relative Gibbs free energy at  $-90^\circ\text{C}$ . The italic values are the values at the B3LYP/6-31+G\* level. The numbers in the structures are bond lengths (Å).

reaction in toluene. The energies were also calculated with Thomasi's polarized continuum model, using the polarizable conductor calculation model [SCRf(CPCM, solvent = THF)]<sup>33</sup> at the corresponding calculation level. The activation energy is reduced by about 11 kcal/mol and **17-pr** is more stable than **17** by about 1 kcal/mol. Furthermore, the transition structures for the lithium–bromine exchange reaction of bromobenzene were located in the presence of one dimethyl ether molecule. The activation energy was reduced by about 13 kcal/mol and **18-pr** is slightly more stable than **18**. These results were similar to the results by the SCRf model in the gas phase (**17**). That is, the bulk of the solvent effect between the substrate and the solvent by the SCRf model is about the same effect for the coordination of one ether solvent to the lithium cation. The application of the SCRf model for **18** reduced the activation energy by about 3 kcal/mol. Since the B3LYP calculations gave almost the same results as the MP2 calculations, the transition structures in the presence of the two dimethyl ether molecules were located at the B3LYP/6-31+G\* level. The activation energy further decreased to 14.1 kcal/mol and the product **19-pr** is more stable than the starting complex **19** by 1.37 kcal/

mol. Thus, the lithium–bromine exchange reaction of bromobenzene with MeLi occurs only in the presence of coordinating solvent. It also should be noted this  $\text{S}_{\text{N}}2$  mechanism (the nucleophilic attack by the methyl anion at the bromine atom) for the lithium–bromine exchange reaction is consistent with Beak's experiments.<sup>20</sup>

## Conclusion

Transition structures for the lithium–halogen exchange reaction of 1,1-dibromoalkenes with both MeLi and MeLi dimer have been located at both MP2/6-31+G\* and B3LYP/6-31+G\* and the kinetic stereoselectivity was predicted correctly by these calculations. That is, the sterically more constrained bromine atoms of 1,1-dibromoalkenes were predominantly reacted with methyllithium in the kinetic condition. The thermodynamic preferences were also predicted correctly by the energy differences of the products. Although both the results obtained from monomeric methyllithium and dimeric methyllithium predict the stereoselectivity correctly, the results obtained with monomeric methyllithium gave better predictions. Furthermore, the effect

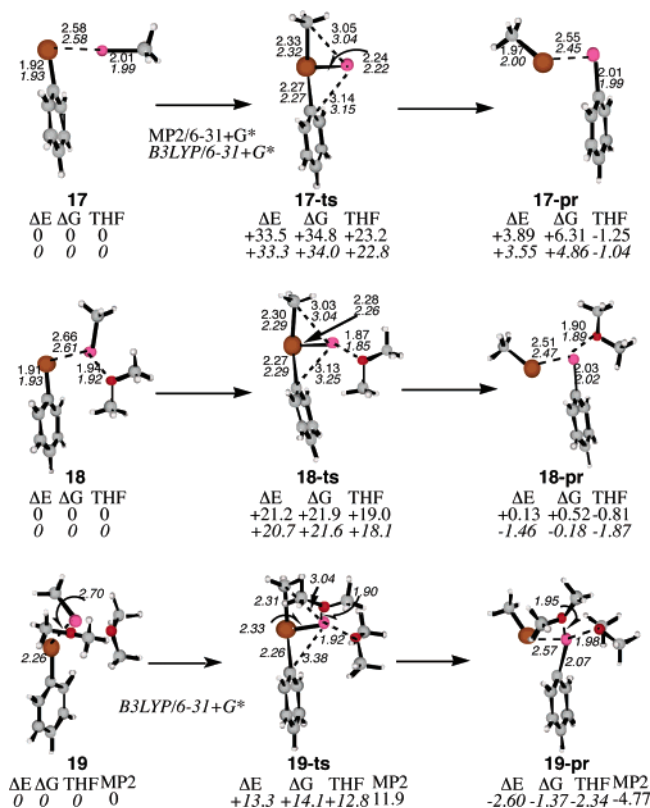


**FIGURE 12.** Transition structures for the lithium–bromine exchange reaction of bromobenzene with methyllithium [MP2/6-31+G\* and B3LYP/6-31+G\*]. ΔG is the relative Gibbs free energy at  $-90^{\circ}\text{C}$ . The THF values are the energies for the SCRf(CPCM,solvent=THF) calculations at the corresponding level. MP2 is the relative energy at the MP2/6-31+G\*//B3LYP/6-31+G\* level.

of coordinating solvent was studied. In the presence of dimethyl ether, the activation energy of the lithium–bromine exchange reaction of dibromoalkene decreases and the C–Br bond in  $\alpha$ -bromo alkenyllithium product was strengthened.

The nucleophilic substitution reaction of  $\alpha$ -halo alkenyllithium compounds occurs easily. In the intramolecular cyclization reaction of lithium 4-bromo-4-lithio-3-methyl-3-pentenoxyde, the driving force is the Li–Br interaction rather than the nucleophilic attack of the oxyanion and the intramolecular substitution reaction proceeds in a concerted manner. Indene formation from 3-(*o*-bromophenyl)-1,1-dibromo-1-propenes in the presence of butyllithium occurs in a similar manner.

The nucleophilic substitution of 1-chloro-2-methylpropenyllithium with monomeric methyllithium or dimeric methyllithium was also studied computationally. The calculations for the reaction with monomeric methyllithium gave better predictions for the experimental stereospecificity rather than those with the dimeric one.

**Acknowledgment.** The generous allotment of computational time (NEC SX-7 computer) from the Institute for Molecular Science, Okazaki, Japan, is deeply acknowledged.

JO0519662